Fission Fragment Intrinsic Spins and Their Correlations

Aurel Bulgac,[1] Ibrahim Abdurrahman,[1] Shi Jin,[1] Kyle Godbey,[2] Nicolas Schunck,[3] and Ionel Stetcu[4]
[1]Department of Physics, University of Washington, Seattle, Washington 98195–1560, USA
[2]Cyclotron Institute, Texas A&M University, College Station, Texas 77843, USA
[3]Lawrence Livermore National Laboratory, Nuclear and Chemical and Sciences Division, Livermore, California 94551, USA
[4]Los Alamos National Laboratory, Theoretical Division, Los Alamos, New Mexico 87545, USA

(Received 24 December 2020; revised 5 February 2021; accepted 11 March 2021; published 7 April 2021)

The intrinsic spins and their correlations are the least understood characteristics of fission fragments from both theoretical and experimental points of view. In many nuclear reactions, the emerging fragments are typically excited and acquire an intrinsic excitation energy and an intrinsic spin depending on the type of the reactions and interaction mechanism. Both the intrinsic excitation energies and the fragments' intrinsic spins and parities are controlled by the interaction mechanism and conservations laws, which lead to their correlations and determines the character of their deexcitation mechanism. We outline here a framework for the theoretical extraction of the intrinsic spin distributions of the fragments and their correlations within the fully microscopic real-time density-functional theory formalism and illustrate it on the example of induced fission of ^{236}U and ^{240}Pu, using two nuclear energy density functionals. These fission fragment intrinsic spin distributions display new qualitative features previously not discussed in literature. Within this fully microscopic framework, we extract for the first time the intrinsic spin distributions of fission fragments of ^{236}U and ^{240}Pu as well as the correlations of their intrinsic spins, which have been debated in literature for more than six decades with no definite conclusions so far.

DOI: 10.1103/PhysRevLett.126.142502

In nuclear reactions, a transient system is formed, which may reach statistical equilibrium as in the case of Bohr's compound nucleus [1] or may only survive for a time shorter than that required to reach statistical equilibrium. The nature of the transient system varies widely, depending on the nature and individual characteristics of the colliding partners, their initial quantum numbers and collision energies, and the conservation laws that always control the evolution of the system and the nature of the final reaction products. As a rule, the final products do not emerge with well-defined quantum numbers such as particle number, intrinsic spins, isospins, parities, linear momenta, or intrinsic energies. Understanding and being able to evaluate the mass and charge fragments yields, their final kinetic energies, their intrinsic excitation energy sharing mechanism, the intrinsic spins and their correlations, and the decay mechanism of the emerging primary products are of outmost interest for understanding the reaction mechanism and for technological applications as well. In particular, the intrinsic energy distributions and their intrinsic spin distributions will determine how the primary reaction or fission products deexcite and emit various other particles. If well-equilibrated fragments are produced, then well-established statistical arguments can be used [2–13].

Intrinsic spin distributions of primary fission fragments (FFs) cannot be directly assessed in the laboratory; they control the neutron and γ-emission spectra and, consequently, a significantly fraction of the energy released in fission. The correlations between the intrinsic spins of the emerging primary FF, in particular, has been a source of a debate, driven by models, remaining unsettled for more than six decades [7,8,14–26]. The scission mechanism is still not fully elucidated and both phenomenological models and incomplete microscopic models, often based on conflicting theoretical assumptions about the character of the large amplitude collective motion [27–30], lead to similar predictions for the fission yields distributions. The current implementation of the time-dependent density-functional theory (TDDFT) extended to superfluid systems [31,32] has proven capable of providing answers to a wide number of problems in cold atom physics, quantum turbulence in fermionic superfluids, vortex dynamics in neutron star crust, and nuclear fission and reactions. The density-functional theory (DFT) and the Schrödinger descriptions are mathematically identical for one-body densities [33–35], with the proviso that in nuclear physics neither the nuclear energy density functional (NEDF) nor the internucleon forces are known with sufficient accuracy yet.

At scission (and immediately after) the FFs are still interacting and can still exchange energy and linear and angular momentum [36]. These processes can lead to various relative excitation modes of the FFs known as axial rotation-tilting, twisting, wriggling, and bending, the existence and importance of which is still a matter of

mostly abstract debate, as a direct and unequivocal experimental proof of their existence and relevance is still lacking. Even if an experimental confirmation of their existence and relevance may prove hard to find, a firm microscopic evidence of the existence of these modes, rooted in a fully quantum treatment may, however, be achieved. We present here a theoretical framework, which allows us to extract the FF intrinsic spin distributions and as well as their correlations, which can shed light for the first time on the existence and nature of these long speculated axial rotation-tilting, twisting, wriggling, and bending modes, with the latter two being doubly degenerate.

We performed TDDFT calculations of ^{236}U and ^{240}Pu using two different NEDFs, SkM* [37] and SeaLL1 [38], in simulation boxes $30^2 \times 60$ with a lattice constant $l = 1$ fm and a corresponding momentum cutoff $p_{\rm cut} = \pi\hbar/l \approx 600$ MeV/c, using the LISE package as described in Refs. [29,39–43]. The initial nuclear wave function Φ was evolved in time from various initial deformations Q_{20} and Q_{30} of the mother nucleus near the outer saddle until the FFs were separated by more than 30 fm as in Refs. [29,43]. Our simulations have a number of significant differences from previous phenomenological and restricted microscopic studies available in literature. (i) There are no assumptions, apart from initial axial symmetry of the fissioning nucleus, or restrictions imposed on the time evolution of the fissioning nucleus and of the emergent FFs. However, we have shown that allowing for initial states with small nonaxial symmetry does not lead to major changes in the final properties of the FFs (see Sec. 3.5.3 in Ref. [41]). Collective rotations and shape vibrations of the mother nucleus that contribute to quantum fluctuations are beyond DFT [40] and are not taken into account in TDDFT. Since the initial fissioning nucleus is deformed, it also rotates, but with a very large rotational period $T_{\rm rot} \approx 3 \times 10^4$ fm/c, which is much longer than the time the nucleus spends from saddle to scission $T_{\rm s2s} = \mathcal{O}(10^3)$ fm/c, and therefore the intrinsic nuclear shape has relatively little time to rotate significantly away from the fission direction. $T_{\rm rot}$ in the initial state can be estimated from the energy of the first rotational state 2^+ of ^{236}U, $\Delta E/\Delta J \approx \hbar\omega = 2\pi\hbar/T_{\rm rot} \approx 40$ keV. Moreover, while evolving from the ground state shape toward the outer fission barrier, the nucleus elongates, its moment of inertia increases considerably, and leads to an even longer rotational period. (ii) We study the stability of our results with respect to varying the nuclear density functionals and the properties of the final FF intrinsic spin distributions appear stable. As we stressed in our previous publications [29,43], the results of these simulations are surprisingly stable with varying the parameters of the nuclear energy density functionals, in good agreement with observations, without any attempts of fitting parameters. (iii) We make no assumptions about the properties of the emerging FFs, their "average properties" are noticeably different from their phenomenologically prescribed or equilibrium properties, and they are defined only after full separation. (iv) The FF shapes have enough time to relax, as we follow them long in time after scission and the FF large amplitude collective motion is also strongly dissipative.

As soon as the FFs are well separated [29,43], it is safe to assume that the FF intrinsic spins are not evolving anymore, see Fig. 1(a). The intrinsic spin of a FF is evaluated then as [41,44,45] $\boldsymbol{J}^F = \int dxdy\psi^\dagger(x)\psi(y)\langle x|\boldsymbol{j}^F|y\rangle$ with $\langle x|\boldsymbol{j}^F|y\rangle = \langle x|\Theta^F(\boldsymbol{r})[(\boldsymbol{r}-\boldsymbol{R}^F)\times(\boldsymbol{p}-m\boldsymbol{v}^F)+\boldsymbol{s}]\Theta^F(\boldsymbol{r})|y\rangle$,

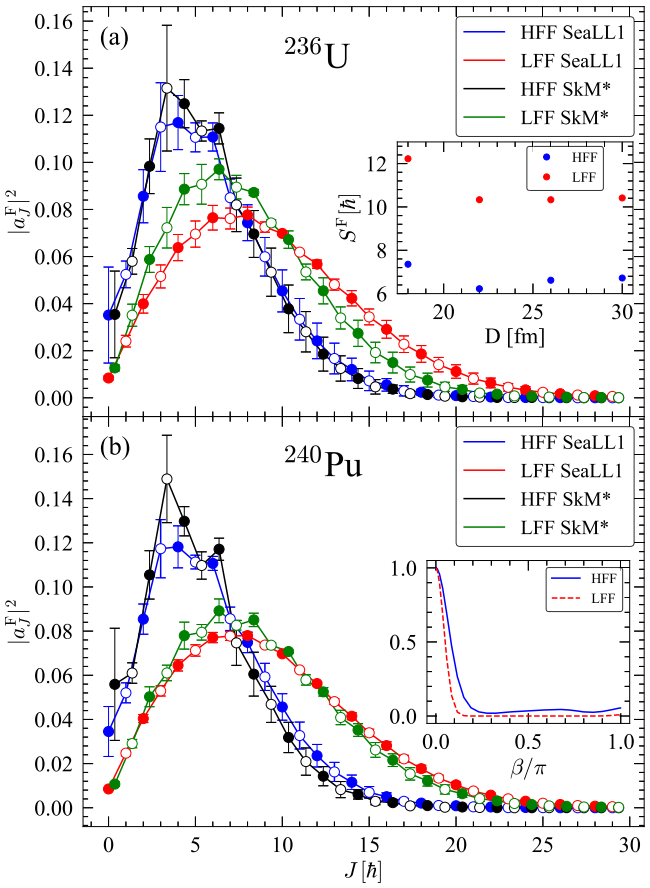

FIG. 1. Values of $|a_J^F|^2$ averaged over initial multipole moments Q_{20}, Q_{30} from the even J^F momenta are displayed with filled symbols, while the contributions arising from odd J^F momenta are displayed with empty symbols. The "error bars" characterize the range of the variation due to the spread of initial multipole moments Q_{20} and Q_{30} and energies of the fissioning nucleus. The $|a_J^F|^2$ for the SeaLL1 [38] and SkM* [37] (displaced by $\Delta J^F = 0.36$ for better visualization) NEDFs are displayed with filled and empty symbols for the even and odd values of J, respectively. The average (standard deviation) for ^{240}Pu are $[A^L, Z^L] = [103.6(0.7), 41.0(0.3)]$ and ^{236}U [102.4(2.0), 40.4(0.7)] in case of SeaLL1 and [104.3(1.5), 41.4(0.5)] and [97.9(1.2), 38.9(0.4)] in case of SkM*, respectively. The evaluated FF intrinsic spins $S^{H,L}$ at different FF separations are shown in the inset for ^{236}U. Typical behavior of the overlaps $\langle\Phi|\hat{R}_x^F(\beta)|\Phi\rangle$ for one TDDFT trajectory is shown in the inset for ^{240}Pu. The overlaps' widths narrow with increasing β and the average S^F increases.

and where $\int dxdy$ stands for integral over 3D spatial coordinates and sum over spin-isospin components, $F = L, H$ (light, heavy), $\boldsymbol{r}$ and $\boldsymbol{p}$ are the nucleon coordinate and momentum, $\boldsymbol{s}$ is its spin, m is the nucleon mass, $\boldsymbol{R}^F$ and $\boldsymbol{v}^F$ are the center of mass and the center of mass velocity of the respective FF, and $\Theta^F(\boldsymbol{r}) = 1$ only in a finite volume centered around that FF, and otherwise $\Theta^F(\boldsymbol{r}) \equiv 0$. In Ref. [44], the fragment apparently was not brought into its own rest frame of reference. In Fig. 1, we show the extracted FF spin distributions $|a_J^F|^2 = (2J+1)/2 \int_0^\pi d\beta \sin\beta P_J(\cos\beta)\langle\Phi|\hat{R}_x^F(\beta)|\Phi\rangle$ with $\sum_{J=0}^\infty |a_J^F|^2 = 1$, $\hat{R}_x^F(\beta) = \exp(-i\hat{J}_x^F\beta/\hbar)$, $P_J(\cos\beta)$ the Legendre polynomials, and assuming that z is the fission direction [45–47]. Like the initial state, the FFs have axial symmetry in our simulations. The presence of the projection on the FF spatial region and on its own reference frame is formally equivalent to introducing a reduced density matrix when evaluating the entanglement entropy [45].

There are a number of new qualitative aspects in our results when compared to previous either phenomenological or restricted microscopic studies [7,8,14–26]. Notice that the spins $\boldsymbol{J}^F$ in Fig. 1 are not restricted to even values of J, as in Ref. [47]. In the absence of reflection symmetry and/or in the presence of currents, the overlap lacks the symmetry $\langle\Phi|\hat{R}_x^F(\beta)|\Phi\rangle = \langle\Phi|\hat{R}_x^F(\pi-\beta)|\Phi\rangle$, and thus for odd J values $|a_J|^2 \neq 0$. (Note that for a spherical nucleus $\langle\Phi|\hat{R}_x(\beta)|\Phi\rangle \equiv 1$, $|a_0|^2 \equiv 1$, and $|a_{J\neq 0}|^2 \equiv 0$.) This is reflected in the aspect of the overlap $\langle\Phi|\hat{R}_x^F(\beta)|\Phi\rangle$, which has a prominent peak at $\beta = 0$ and an almost Gaussian shape, see inset in Fig. 1(b). As Scamps and Simenel [48] have noticed and was also observed by us [29,39,43] in independent calculations with different NEDFs and different implementation of TDDFT, FFs emerge with nonvanishing octupole deformations. The light FFs (LFFs) are extremely elongated when the FFs are well separated with $\beta_2^L \approx 5, \ldots, 10\beta_2^H$, see Table I. It is not surprising that the open shell LFFs have large deformations and thus can sustain quite large collective angular momenta, unlike the heavy FFs (HFFs). For decades in literature, it was stated that the mass and charge of the HFF is correlated with its proximity to the magic nucleus, typically ^{132}Sn or ^{208}Pb in the case of fission of superheavy elements, and with a strong role of the shell effects [49,50]. Since the HFFs are always close to the magic ^{132}Sn nucleus, their deformations are smaller than those of the LFFs, a fact reflected in the character of the overlaps $\langle\Phi|\hat{R}_x^F(\beta)|\Phi\rangle$ and by the evaluated primary FFs spins. This is at odds with phenomenological inferences that the HFFs can carry a larger intrinsic spin, and doubts about the veracity of such an assumption have been raised for quite some time [24]. At large separations, the octupole moments of both FFs are relatively small, $\beta_3^L = 0.00, \ldots, 0.02(0.02, \ldots, 0.07)$ and $\beta_3^H = -0.05, \ldots, 0.09(0.01, \ldots, 0.03)$. The maximum and the range of the collective spin a nucleus can sustain are larger for more deformed nuclei [46,51].

TABLE I. The averages (standard deviations) of S^F and of β_2^F are evaluated over the set of initial conditions, where for each FF $\beta_\lambda^F = 4\pi \int d^3r n^F(\boldsymbol{r}) r^\lambda Y_{\lambda 0}(\hat{\boldsymbol{r}})/[3A(1.2A^{1/3})^\lambda]$, where $n^F(\boldsymbol{r})$ is the FF intrinsic density. The FF $\beta_3^L = 0.00, \ldots, 0.02(0.02, \ldots, 0.07)$ and $\beta_3^H = -0.09, \ldots, -0.04(0.01, \ldots, 0.03)$ are noticeably smaller.

Nucleus	NEDF	S^L	S^H	β_2^L	β_2^H
^{236}U	SeaLL1	10.5 (0.6)	6.8(0.7)	0.67(0.07)	0.09(0.04)
^{236}U	SkM*	8.6(0.6)	6.3(0.7)	0.46(0.10)	0.09(0.03)
^{240}Pu	SeaLL1	10.4(0.3)	6.7(0.5)	0.62(0.04)	0.06(0.03)
^{240}Pu	SkM*	9.4(0.4)	5.8(0.5)	0.54(0.06)	0.06(0.03)

There are clear odd-even J effects in the $|a_J|^2$ distributions, and the odd values of J are slightly suppressed when compared to the neighboring even values of J. One should remember that we did not perform FF particle number projections and these odd-even effects appear for the "average even-even" FFs. The distributions $|a_J^H|^2$ of the HFF show a prominent two peak structure. An additional feature is a rather prominent enhancement of the average value of $P(0)$ in case of the HFF, larger than expected value of $|a_0|^2$, when compared to a statistical approach distribution [15–20,24], and also as seen from the significant error bar of $|a_0|^2$. The gross features of the spin distributions obtained within TDDFT, see Fig. 1, can be reasonably well reproduced with phenomenological-statistical approach formula $|a_J|^2 \propto (2J+1)\exp[-J(J+1)/2\sigma^2]$, where σ is typically a fitting parameter. For each set of initial conditions Q_{20}, Q_{30}, as described in Refs. [29,39–43], we have extracted the values of S^F for each FF from the corresponding $|a_J^F|^2$ distribution $S^F(S^F+1) = \sum_J J(J+1)|a_J^F|^2$, and then we evaluated their averages and standard deviation over the initial conditions Q_{20}, Q_{30}, see Table I. The SeaLL1 NEDF leads to a bit wider spin distributions than the SkM* NEDF, but otherwise to comparable widths. The even-odd effects are more pronounced in the case of SkM* NEDF and, particularly, in the case of LFF, due likely to its reduced effective nucleon mass, and emerges with a noticeable octupole deformation [29,39,42,43,48].

The correlation between the intrinsic spins of two FFs $\langle\Phi|J_\alpha^L J_\beta^H|\Phi\rangle = \langle\Phi|J_\beta^H J_\alpha^L|\Phi\rangle$ reveals information about the FF dynamics at and after scission. By determining the principal axes of the tensor $\langle\Phi|J_\alpha^L J_\beta^H|\Phi\rangle$ and the corresponding eigenvalues, one can disentangle and characterize the relevance of the axial rotation-tilting, wriggling, twisting, and bending modes [8,13,14,17,21–23,26]. Since $\langle\Phi|J_\alpha^L J_\alpha^H|\Phi\rangle < 0$, we confirm the presence of the bending and twisting modes in fission, with the bending mode being double degenerate, as expected. These conclusions are based for the first time on a detailed

TABLE II. The averages (standard deviations) of $\langle\Phi|J^L_\alpha J^H_\alpha|\Phi\rangle$, with $\alpha = x, y, z$. The nondiagonal elements of this tensor are negligible and all $\langle\Phi|J^F_\alpha|\Phi\rangle = 0$.

Nucleus	NEDF	$\langle\Phi\|J^L_x J^H_x\|\Phi\rangle$	$\langle\Phi\|J^L_y J^H_y\|\Phi\rangle$	$\langle\Phi\|J^L_z J^H_z\|\Phi\rangle$
^{236}U	SeaLL1	−1.16(0.63)	−1.16(0.63)	−2.63(0.47)
^{236}U	SkM*	−0.48(0.71)	−0.48(0.71)	−1.62(0.30)
^{240}Pu	SeaLL1	−0.72(0.65)	−0.72(0.65)	−4.43(0.92)
^{240}Pu	SkM*	−0.90(0.57)	−0.90(0.57)	−1.80(0.52)

microscopic description of the fission process in a quantum mechanical real-time many-body treatment, without any assumptions and with no restrictions at the mean field level, in contradistinction with previous phenomenological models or restricted microscopic studies. We cannot exclude, however, the presence to some (small) admixture of axial rotation-tilting and wriggling, corresponding to FF rotations around the fission direction and perpendicular to the fission direction, respectively, likely due to fluctuations and/or the presence of $K \neq 0$ components.

It is instructive to qualitatively analyze these results in the semiclassical limit. From data in Tables I and II, it follows that the FF intrinsic spins are on average orthogonal to each other, as the value of cosine of their angle is small $\cos\phi^{LH} = \langle\Phi|\boldsymbol{J}^L \cdot \boldsymbol{J}^H|\Phi\rangle/J^L J^H \approx 0.1$. (For two random vectors, the cosine would be $0 \pm 1/\sqrt{3}$.) As the total angular momentum is conserved $\boldsymbol{J}_0 = \boldsymbol{J}^L + \boldsymbol{J}^H + \boldsymbol{L}$ and $J^{L,H}_z = L_z = 0$, these angular momenta are all approximately perpendicular to the fission direction z. After introducing the total intrinsic FF spin $\boldsymbol{J} = \boldsymbol{J}^L + \boldsymbol{J}^H$, one finds that $J \approx 12, \ldots, 13$. At $E'_n \approx 20$ MeV, according to the analysis performed in Ref. [13] in case of ^{235}U(n,f), the angular momentum brought in by the neutron can reach $\approx 5\hbar$, and thus J_0 can reach values comparable to J and L. As the ground state spins of ^{239}Pu and ^{235}U are $1/2^+$ and $7/2^-$, for slow neutrons the spins of the compound nuclei formed in ^{239}Pu(n,f) and ^{235}U(n,f) reactions are $J_0(^{240}\text{Pu}) = 0^+, 1^+$ and $J_0(^{236}\text{U}) = 3^-, 4^-$, with J_0 noticeably smaller than J and L. Since the rotation of the fission direction is controlled by the moment of inertia $\mathcal{I}_R = M^H M^L R^2/(M^H + M^L) \to \infty$, where $M^{L,H}$ are the FF masses and R is their separation, this rotation angle is expected to be relatively small.

In the case of ^{240}Pu, we have performed additional simulations with the NEDF SkM* by varying the equivalent incident neutron energy in reaction ^{239}Pu(n,f), thus simulating a compound nucleus ^{240}Pu with various excitation energies E^*, see Fig. 2. With increasing E_n, the intrinsic spin of the HFF shows a significant increase, which correlates with the steeper increase of the HFF excitation energy E^H_{int} when compared to the behavior of the LFF excitation energy E^L_{int}. Nevertheless, in this entire energy interval, the HFF temperature remains lower than the LFF temperature on average.

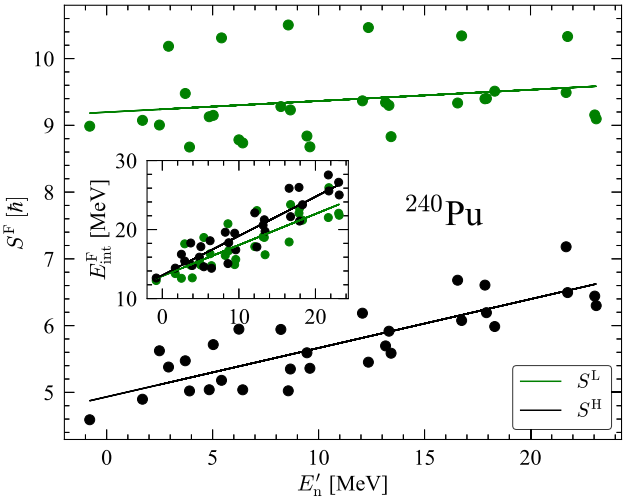

FIG. 2. The average intrinsic spins $S^{L,H}$ versus the initial FF equivalent incident neutron energy $E'_n = E^* - S_n$ (E^* and S_n are the excitation energy and S_n is the neutron separation energy) for the reaction ^{239}Pu(n,f) with SkM* NEDF. The solid lines are linear fits over the data, $S^L = 0.0168E'_n + 9.197$ and $S^H = 0.0732E'_n + 4.933$, respectively, as a function of equivalent neutron energy E'_n along with their linear fits. Inset: the FF excitation energies and their linear fits $E^L_{\text{int}} = 0.4505E'_n + 13.25$ and $E^H_{\text{int}} = 0.5676E'_n + 13.40$. Using $E^F_{\text{int}} \approx A^F(T^F)^2/10$ [43,51], it follows that, on average, $T^L > T^H$.

A recent constrained Hartree-Fock-Bogoliubov evaluation of the FF intrinsic spins [52], using prescission configurations with the same A^L and Z^L as the final FF values obtained in TDDFT calculations from different initial conditions [45], arrived at similar results to these reported here, provided the neck thickness at rupture is chosen small enough. As the FF deformations and excitation energies change significantly after scission [29,43] and the FF moments of inertia which are $\propto \beta_2^2$ [46], the intrinsic spin distributions change with FF separation, see Fig. 1(a). We have compared the default CGMF results [6,7,9,10,12] for the γ spectra with those obtained by using instead the microscopic intrinsic spin distributions. While fewer average number of gammas were produced when the microscopic parametrization was employed, we have not observed large changes for the prompt fission γ spectrum. One should keep in mind that the CGMF model is based on a large number of phenomenological parameters. In the CGMF approach, one assumes that $J^H > J^L$, opposite to our conclusions. This assumption is hard to reconcile with the fact that the HFF has a relatively modest deformation. In another study [13], within the phenomenological model FREYA, one finds that FF intrinsic antiparallel intrinsic spins show a slight preference. Using our language, the expected average of $\langle\Phi|J^L_\alpha J^H_\alpha|\Phi\rangle$ for $\alpha = x, y$ is negative, in qualitative agreement with our results. In FREYA, the intrinsic spin fluctuations are controlled by the temperature

of the fissioning nucleus at scission. According to our earlier results [29,43], the FF deformations at scission and their relaxed values are very different, with larger deformations at scission and with the HFF cooler than the LFF, while FREYA assumes identical temperatures. While within the FREYA framework, the "thermal" intrinsic spin fluctuations dominate over their averages and these authors find that average difference $|S^H - S^L| \approx 1, \ldots, 2$ is smaller than our values. Since in FREYA the FF moments of inertia are $\mathcal{I}^H > \mathcal{I}^L$, it immediately follows that $S^H > S^L$, opposite to our results. At the same time, FREYA finds S^H values and an increase in $S^{L,H}$ with the excitation energy of the compound fissioning nucleus qualitatively similar to our findings, see Fig. 2. In FREYA, the axial rotation-tilting and twisting modes are suppressed [22], while we find that magnitude of $\langle\Phi|J_z^L J_z^H|\Phi\rangle$ is larger than $\langle\Phi|J_\alpha^L J_\alpha^H|\Phi\rangle$ for $\alpha = x, y$.

We have demonstrated that TDDFT allows one to extract detailed microscopic information about the FF intrinsic spins, their dependence on excitation energy of the compound nucleus, and the FF intrinsic spin correlations, which are almost impossible to infer unambiguously from phenomenological analyses.

A. B. thanks G. F. Bertsch for discussions. We also want to express our gratitude to K. J. Roche for enthusiastically sharing with us his insights into effectively using supercomputers. A. B. was supported by U.S. Department of Energy, Office of Science, Award No. DE-FG02-97ER41014, and in part by NNSA Cooperative Agreement No. DE-NA0003841. The work of N. S. was supported by the Scientific Discovery through Advanced Computing (SciDAC) program funded by the U.S. Department of Energy, Office of Science, Advanced Scientific Computing Research and Nuclear Physics, and it was partly performed under the auspices of the U.S. Department of Energy by the Lawrence Livermore National Laboratory under Award No. DE-AC52-07NA27344. The work of I. S. was supported by the U.S. Department of Energy through the Los Alamos National Laboratory. Los Alamos National Laboratory is operated by Triad National Security, LLC, for the National Nuclear Security Administration of U.S. Department of Energy (Award No. 89233218CNA000001). I. S. gratefully acknowledges partial support by the Laboratory Directed Research and Development program of Los Alamos National Laboratory under Project No. 20200384ER and partial support and computational resources provided by the Advanced Simulation and Computing (ASC) Program. This material (work of A. B., I. A., and K. G.) is partially based upon work supported by the Department of Energy, National Nuclear Security Administration, under Award No. DE-NA0003841. Some of the calculations reported here have been performed with computing support from the Lawrence Livermore National Laboratory (LLNL) Institutional Computing Grand Challenge program. This research used resources of the Oak Ridge Leadership Computing Facility, which is a U.S. DOE Office of Science User Facility supported under Award No. DE-AC05-00OR22725 and of the National Energy Research Scientific Computing Center, which is supported by the Office of Science of the U.S. Department of Energy under Award No. DE-AC02-05CH11231. We acknowledge PRACE for awarding us access to resource Piz Daint based at the Swiss National Supercomputing Centre (CSCS), decision No. 2018194657. This work is supported by "High Performance Computing Infrastructure" in Japan, Project ID: hp180048. A series of simulations were carried out on the Tsubame 3.0 supercomputer at Tokyo Institute of Technology. This research used resources provided by the Los Alamos National Laboratory Institutional Computing Program. A. B. devised the theoretical framework. I. A., S. J., and I. S. performed TDDFT calculations and I. A., K. G., and I. S. implemented and performed the extraction of the spin distributions. N. S. performed the calculations of the initial configurations for the TDDFT simulations. All authors participated in the discussion of the results and the writing of the Letter.

[1] N. Bohr, Neutron capture and nuclear constitution, Nature (London) **137**, 344 (1936); **137**, 351 (1936).
[2] V. Weisskopf, Statistics and nuclear reactions, Phys. Rev. **52**, 295 (1937).
[3] W. Hauser and H. Feshbach, The inelastic scattering of neutrons, Phys. Rev. **87**, 366 (1952).
[4] R. Vogt, J. Randrup, D. A. Brown, M. A. Descalle, and W. E. Ormand, Event-by-event evaluation of the prompt fission neutron spectrum from ^{239}Pu(n, f), Phys. Rev. C **85**, 024608 (2012).
[5] R. Vogt and J. Randrup, Event-by-event modeling of prompt neutrons and photons from neutron-induced and spontaneous fission with FREYA, Phys. Procedia **47**, 82 (2013).
[6] I. Stetcu, P. Talou, T. Kawano, and M. Jandel, Isomer production ratios and the angular momentum distribution of fission fragments, Phys. Rev. C **88**, 044603 (2013).
[7] B. Becker, P. Talou, T. Kawano, Y. Danon, and I. Stetcu, Monte Carlo Hauser-Feshbach predictions of prompt fission γ rays: Application to $n_{\text{th}} + ^{235}$U, $n_{\text{th}} + ^{239}$Pu, and ^{252}Cf (sf), Phys. Rev. C **87**, 014617 (2013).
[8] J. Randrup and R. Vogt, Refined treatment of angular momentum in the event-by-event fission model FREYA, Phys. Rev. C **89**, 044601 (2014).
[9] I. Stetcu, P. Talou, T. Kawano, and M. Jandel, Properties of prompt-fission γ rays, Phys. Rev. C **90**, 024617 (2014).
[10] P. Talou, R. Vogt, J. Randrup, M. E. Rising, S. A. Pozzi, J. Verbeke, M. T. Andrews, S. D. Clarke, P. Jaffke, M. Jandel, T. Kawano, M. J. Marcath, K. Meierbachtol, L. Nakae, G. Rusev, A. Sood, I. Stetcu, and C. Walker, Correlated prompt fission data in transport simulations, Eur. Phys. J. A **54**, 9 (2018).
[11] J. Randrup, P. Talou, and R. Vogt, Sensitivity of neutron observables to the model input in simulations of ^{252}Cf(sf), Phys. Rev. C **99**, 054619 (2019).

[12] P. Talou, I. Stetcu, P. Jafke, M. E. Rising, A. E Lovell, and T. Kawano, Cascading gamma-ray multiplicity and fission, open source code: https://www.github.com/lanl/cgmf.

[13] R. Vogt and J. Randrup, Angular momentum effects in fission, Phys. Rev. C **103**, 014610 (2021).

[14] V. M. Strutinsky, Angular anisotropy of gamma quanta that accompany fission, Sov. Phys. JETP **10**, 613 (1960), http://jetp.ac.ru/cgi-bin/e/index/e/10/3/p613?a=list.

[15] J. R. Huizenga and R. Vandenbosch, Interpretation of isomeric cross-section ratios for (n, γ) and (γ, n) reactions, Phys. Rev. **120**, 1305 (1960).

[16] R. Vandenbosch and J. R. Huizenga, Isomeric cross-section ratios for reactions producing the isomeric pair $hg^{197,197m}$, Phys. Rev. **120**, 1313 (1960).

[17] J. R. Nix and W. J. Swiatecki, Studies in the liquid-drop theory of nuclear fission, Nucl. Phys. **71**, 1 (1965).

[18] J. O. Rasmussen, W. Nörenberg, and H. J. Mang, A model for calculating the angular momentum distribution of fission fragments, Nucl. Phys. **A136**, 465 (1969).

[19] J. B. Wilhelmy, E. Cheifetz, R. C. Jared, S. G. Thompson, H. R. Bowman, and J. O. Rasmussen, Angular momentum of primary products formed in the spontaneous fission of ^{252}Cf, Phys. Rev. C **5**, 2041 (1972).

[20] R. Vandenbosch and J. R. Huizenga, *Nuclear Fission* (Academic Press, New York, 1973).

[21] L. G. Moretto and R. P. Schmitt, Equilibrium statistical treatment of angular momenta associated with collective modes in fission and heavy-ion reactions, Phys. Rev. C **21**, 204 (1980).

[22] T. Døssing and J. Randrup, Dynamical evolution of angular momentum in damped nuclear reactions: (I). Accumulation of angular momentum by nucleon transfer, Nucl. Phys. **A433**, 215 (1985).

[23] L. G. Moretto, G. F. Peaslee, and G. J. Wozniak, Angular-momentum-bearing modes in fission, Nucl. Phys. **A502**, 453c (1989).

[24] *The Nuclear Fission Process*, edited by C. Wagemans (CRS Press, Boca Raton, FL, 1991).

[25] L. Bonneau, P. Quentin, and I. N. Mikhailov, Scission configurations and their implication in fission-fragment angular momenta, Phys. Rev. C **75**, 064313 (2007).

[26] R. Vogt and J. Randrup, Event-by-event study of photon observables in spontaneous and thermal fission, Phys. Rev. C **87**, 044602 (2013).

[27] J. K. Krappe and K. Pomorski, *Theory of Nuclear Fission* (Springer, Heidelberg, 2012).

[28] N. Schunck and L. M. Robledo, Microscopic theory of nuclear fission: A review, Rep. Prog. Phys. **79**, 116301 (2016).

[29] A. Bulgac, S. Jin, and I. Stetcu, Nuclear fission dynamics: Past, present, needs, and future, Front. Phys. **8**, 63 (2020).

[30] M. Bender, R. Bernard, G. Bertsch, S. Chiba, J. Dobaczewski, N. Dubray, S. A. Giuliani, K. Hagino, D. Lacroix, Z. Li, P. Magierski, J. Maruhn, W. Nazarewicz, J. Pei, S. Péru, N. Pillet, J. Randrup, D. Regnier, P.-G. Reinhard, L. M. Robledo, W. Ryssens, J. Sadhukhan, G. Scamps, N. Schunck, C. Simenel, J. Skalski, I. Stetcu, P. Stevenson, S. Umar, M. Verriere, D. Vretenar, M. Warda, and S. Åberg, Future of nuclear fission theory, J. Phys. G **47**, 113002 (2020).

[31] A. Bulgac, Time-dependent density functional theory and the real-time dynamics of fermi superfluids, Annu. Rev. Nucl. Part. Sci. **63**, 97 (2013).

[32] A. Bulgac, Time-dependent density functional theory for fermionic superfluids: From cold atomic gases, to nuclei and neutron star crust, Phys. Status Solidi B **256**, 1800592 (2019).

[33] R. M. Dreizler and E. K. U. Gross, *Density Functional Theory: An Approach to the Quantum Many–Body Problem* (Springer-Verlag, Berlin, 1990).

[34] *Time-Dependent Density Functional Theory*, edited by M. A. L. Marques, C. A. Ullrich, F. Nogueira, A. Rubio, K. Burke, and E. K. U. Gross, Lecture Notes in Physics Vol. 706 (Springer-Verlag, Berlin, 2006).

[35] *Fundamentals of Time-Dependent Density Functional Theory*, edited by M. A. L. Marques, N. T. Maitra, F. M. S. Nogueira, E. K. U. Gross, and A. Rubio, Lecture Notes in Physics Vol. 837 (Springer, Heidelberg, 2012).

[36] A. Bulgac, Fission-fragment excitation energy sharing beyond scission, Phys. Rev. C **102**, 044609 (2020).

[37] J. Bartel, P. Quentin, M. Brack, C. Guet, and H.-B. Håkansson, Towards a better parametrisation of Skyrme-like effective forces: A critical study of the SkM force, Nucl. Phys. **A386**, 79 (1982).

[38] A. Bulgac, M. McNeil Forbes, S. Jin, R. N. Perez, and N. Schunck, Minimal nuclear energy density functional, Phys. Rev. C **97**, 044313 (2018).

[39] A. Bulgac, P. Magierski, K. J. Roche, and I. Stetcu, Induced Fission of ^{240}Pu Within a Real-Time Microscopic Framework, Phys. Rev. Lett. **116**, 122504 (2016).

[40] A. Bulgac, S. Jin, and I. Stetcu, Unitary evolution with fluctuations and dissipation, Phys. Rev. C **100**, 014615 (2019).

[41] S. Jin, I. Roche, K. J. Stetcu, I Abdurrahman, and A. Bulgac, The LISE package: Solvers for static and time-dependent superfluid local density approximation equations in three dimensions, arXiv:2009.00745.

[42] I. Abdurahman, A. Bulgac, N. Schunck, and I. Stetcu, Fission fragment properties (to be published).

[43] A. Bulgac, S. Jin, K. J. Roche, N. Schunck, and I. Stetcu, Fission dynamics of ^{240}Pu from saddle to scission and beyond, Phys. Rev. C **100**, 034615 (2019).

[44] K. Sekizawa, Microscopic description of production cross sections including deexcitation effects, Phys. Rev. C **96**, 014615 (2017).

[45] A. Bulgac, Projection of good quantum numbers for reaction fragments, Phys. Rev. C **100**, 034612 (2019).

[46] P. Ring and P. Schuck, *The Nuclear Many-Body Problem*, 1st ed., Theoretical and Mathematical Physics Series Vol. 17 (Springer-Verlag, Berlin, Heidelberg, New York, 2004).

[47] G. F. Bertsch, T. Kawano, and L. M. Robledo, Angular momentum of fission fragments, Phys. Rev. C **99**, 034603 (2019).

[48] G. Scamps and C. Simenel, Impact of pear-shaped fission fragments on mass-asymmetric fission in actinides, Nature (London) **564**, 382 (2018).

[49] V. M. Strutinsky, Shell effects in nuclear masses and deformation energies, Nucl. Phys. **A95**, 420 (1967).

[50] M. Brack, J. Damgaard, A. S. Jensen, H. C. Pauli, V. M. Strutinsky, and C. Y. Wong, Funny hills: The shell-correction approach to nuclear shell effects and its applications to the fission process, Rev. Mod. Phys. **44**, 320 (1972).

[51] A. Bohr and B. R. Mottelson, *Nuclear Structure* (Benjamin, Inc., New York, 1969).

[52] P. Marevic, N. Schunck, J. Randrup, and R. Vogt, Angular momentum of fission fragments from microscopic theory, arXiv:2101.03406.